



Optimization of Ni/ZrO₂ catalytic performance in thermochemical cellulose conversion for enhanced hydrogen production

Agnieszka M. Ruppert^{a,*}, Michał Niewiadomski^a, Jacek Grams^a, Witold Kwapiński^b

^a Institute of General and Ecological Chemistry, Faculty of Chemistry, Lodz University of Technology, ul. Żeromskiego 116, 90-924 Łódź, Poland

^b Carbolea Research Group, Department of Chemical and Environmental Science, University of Limerick, Limerick, Ireland

ARTICLE INFO

Article history:

Received 24 October 2012

Received in revised form 5 January 2013

Accepted 9 January 2013

Available online 22 January 2013

Keywords:

Nickel

Zirconium oxide

Pyrolysis

Biomass

Cellulose

Catalyst

ABSTRACT

Hydrogen and syngas from cellulose or cellulosic biomass gasification are environmentally clean gaseous fuels used for power generation. In this work, we explored the potential of several Ni/ZrO₂ catalysts for the thermochemical conversion of cellulose to hydrogen. From the investigated catalysts the one consisting of tetragonal zirconia and containing the active phase with a small crystallite size and stable surface area, performed best in the cellulose conversion. Migration of zirconia on the nickel surface was found to be beneficial for catalytic performance. According to the XPS results, the highest Zr/Ni ratio was measured on the tetragonal phase of zirconia, followed by monoclinic ZrO₂, with amorphous zirconia showing the lowest migration tendency.

© 2013 Elsevier B.V. All rights reserved.

1. Introduction

Due to the increasing energy demand and climate changes there is a need to use alternative energy sources. It can be realized by developing new synthetic pathways of fuels and chemicals which would be based on lignocellulose as the most abundant second generation biofeedstock [1]. Hydrogen, which is currently mainly produced by natural gas steam reforming, in the future can also be obtained by cellulose valorization. Hydrogen is primarily used in methanol and ammonia syntheses, fuel cells, and hydrogenation reactions. One of the ways which can be applied to the production of gases of major importance in energy sector (H₂, CO) is a pyrolysis or gasification of lignocellulosic biomass [2].

In the biomass valorization, price of the catalytic materials is an important factor, therefore non-noble metal catalysts should be preferably used. Literature data show that nickel has a potential as an attractive, cheap metal catalyst for thermal conversion of biomass towards gases [3]. One of the major problems in gasification or pyrolysis of lignocellulosic feedstock is the formation of tars (condensable organic material) during the reaction. Condensed tar can cause the blocking and fouling of industrial turbines and engines.

Nickel is also considered as one of the best metals for tars elimination due to its ability to catalyze the C–C, C–H and O–H bond

cleavage, which additionally confirms its choice as a metal catalyst [4–7]. However, due to severe conditions during the process (high temperature) catalysts based on Ni usually suffer from fast deactivation caused by rapid carbon deposition and sintering of Ni particles [8]. Their resistance to deactivation can be improved by the modification of surface properties of the used systems, i.e. by the development of a proper catalyst support. It is known that strong interactions between nickel oxide and some supports and high metal dispersion on a large surface area support can mitigate nickel sintering [9].

It is also known that ZrO₂, as a material with equilibrated amount of acidic and basic sites, limits the carbon deposition and possesses very good thermal stability and excellent redox properties [10,11], and the same may be considered an attractive support for Ni in thermal biomass conversion. The beneficial effect of Ni/zirconia was already shown in the literature, where the positive influence of ZrO₂ addition to Ni/Al₂O₃ catalysts was found in hydrogen production from glycerol [12]. Zheng et al. studied Ni/ZrO₂ catalysts in cyclic stepwise methane reforming towards hydrogen and found that by tuning the zirconia properties it is possible to considerably increase the catalytic activity, especially at high reaction temperatures. By application of zirconia nanocomposites they obtained comparably sized Ni and ZrO₂ nanocrystallites. Their sintering could be avoided due to that fact they were able to change the nature of the carbon deposit which was a key to high stability of those materials [13]. Watanabe et al. found that zirconia catalysts can be very efficient in gasification of biomass in supercritical water, thanks to their acid-base properties [14]. It was also reported

* Corresponding author. Tel.: +48 426313106; fax: +48 426313128.

E-mail address: aruppert@p.lodz.pl (A.M. Ruppert).

that by tuning the size of ZrO_2 and Ni crystallites the hydrogen yield in methane reforming can be increased, and also catalyst stability can be improved at high temperatures [13]. On the other hand, low activity of ZrO_2 in some cases could be associated with its low surface area [12,15].

It was also shown in our earlier research [16,17], that from all tested oxides (Al_2O_3 , SiO_2 , CeO_2 , TiO_2 , MgO) ZrO_2 proved to be the most valuable support for Ni catalysts in the thermochemical biomass conversion, as the highest H_2 yield was obtained over commercial Ni/ ZrO_2 . Therefore in this work, we explored the potential of high surface area zirconia obtained by several different methods as an efficient support for nickel catalysts in thermochemical conversion of cellulose to hydrogen. To the best of our knowledge the subject was not investigated so far. Additionally we aim at understanding the nature of catalytic active sites and their influence on the activity enhancement.

2. Experimental

2.1. Catalyst preparation

Zirconium oxides were prepared using several methods described below. The following abbreviations are used in the text:

- ZR-1 was a commercial ZrO_2 material which was used as delivered (Aldrich, 99%).
- ZR-2 was prepared by calcination in air of $\text{ZrO}(\text{NO}_3)_2 \cdot \text{H}_2\text{O}$ (Aldrich, 99% purity) at 400°C for 4 h.
- ZR-3 was prepared by precipitation with Pluronic® P123 (PEG-PPG-PEG) (Aldrich, average Mn ~ 5800) polymer template from $\text{ZrO}(\text{NO}_3)_2$ [18]. First, aqueous solution of P123 and zirconium precursor ($\text{ZrO}(\text{NO}_3)_2 \cdot x\text{H}_2\text{O}$ (Aldrich, 99% purity)) was prepared, with 0.03 M concentration of $\text{ZrO}(\text{NO}_3)_2$ and 0.03 molar ratio of P123 to ZrO_2 . Ammonia (Chempur, 25% concentration, pure for analysis) was then added dropwise to pH = 11 and the mixture was heated to 88°C and stirred for 24 h. The precipitate was filtered on a Büchner funnel and washed with acetone (StanLab, pure for analysis) to remove template polymer residues, and then with water. It was then dried at 110°C in air for 24 h and calcined in air at 500°C for 3 h.
- ZR-4 was prepared by similar precipitation method as described above, only without a polymer template.
- ZR-5 was prepared from ZrOCl_2 (Sigma–Aldrich, pure for analysis ($\geq 99.5\%$)) by precipitation with NaOH followed by calcination at 700°C in air [19]. First, 200 ml of 0.4 M ZrOCl_2 was added dropwise to 60 ml of 5 M NaOH (StanLab, pure for analysis). Then the mixture was heated to 104°C and stirred for 24 h. The precipitate was filtered on a Büchner funnel and washed with 0.05 M solution of NH_4NO_3 (Chempur, pure (min. 99%)) and then with water until neutral pH. It was then dried in air at 110°C overnight and calcined in air at 700°C for 3 h.
- The catalysts were obtained by impregnating the oxides with 1 M $\text{Ni}(\text{NO}_3)_2$ ($\text{Ni}(\text{NO}_3)_2 \cdot 6\text{H}_2\text{O}$ (Chempur, pure for analysis (min. 99%)) aqueous solution to obtain 20 wt.% Ni content calculated for the catalyst amount. Before the reaction the catalysts were calcined in air at 500°C for 4 h, except Ni-ZR-6, which was prepared by high temperature treatment of Ni-ZR-1 at 900°C for 4 h.
- Ni-ZR-X (X = 1–6) are used for the nickel-impregnated catalysts.

Samples which were subjected to characterization ‘after reaction’ were prepared in the same conditions as during reaction but without the presence of cellulose, in order to avoid the influence of other factors like carbon deposit and tar formation.

2.2. Catalyst characterization

Temperature-programmed reduction (TPR) was performed on AMI1 system from Altamira Instruments equipped with a thermal conductivity detector and used for examining the reducibility of the catalysts calcined at 500°C . In the experiments, mixtures of 5 vol.% H_2 and 95 vol.% Ar or 2 vol.% O_2 and 98 vol.% Ar were used at space velocity $3.1 \times 10^{-9} \text{ g s}^{-1} \text{ cm}^{-3}$ and linear temperature ramp of $10^\circ\text{C min}^{-1}$. The surface area was measured by the BET method.

X-ray photoelectron spectroscopy (XPS) surface analysis of the investigated catalysts was performed on Kratos AXIS 165 spectrometer using Al mono $\text{K}\alpha$ X-ray. The samples were fixed onto the sample holder by double-sided adhesive tape.

Powder X-ray diffractograms were collected using a PANalytical X'Pert Pro MPD diffractometer. The X-ray source was a copper long fine focus X-ray diffraction tube operating at 40 kV and 30 mA. Data were collected in the $5\text{--}90^\circ 2\theta$ range with 0.0167° step. Crystalline phases were identified by references to ICDD PDF-2 (ver. 2004) database. All calculations were performed with X'Pert HighScore Plus computer program.

Transmission electron microscope (TEM) – JEM-2100F, JEOL – was used for the measurement of the metal particle size on the surface of the different supports. Prior to TEM analysis, all catalysts were reduced for 1 h at 500°C under hydrogen flow.

2.3. Catalytic activity

The activity tests were performed in a 250 cm^3 stirred batch reactor under atmospheric pressure and $15 \text{ cm}^3 \text{ min}^{-1}$ flow of Ar at 700°C during 4 h. Pyrolysis of α -cellulose (Sigma–Aldrich, pure) as a biomass model (5 g) was conducted both without a catalyst and in the presence of a nickel catalyst (0.2 g). In the case of NiO only 0.04 g of the catalyst was used, which is equivalent of the NiO quantity in the supported systems. Gaseous products were analyzed by gas chromatography (GCHF 18.3, Chromosorb 102 column) equipped with the TCD detector. Besides the gas fraction, the liquid one was also collected. It appeared that the presence of catalysts decreased the amount of condensables in comparison to a reaction without catalyst. For all investigated Ni/zirconia catalysts the composition of liquid phase was similar. Liquid fraction was analyzed by GC–MS.

3. Results

3.1. Catalytic performance

As the aim of our research was to find the optimum Ni/zirconia system which provides the highest hydrogen yield, the focus was on a formation of light gaseous reaction products (H_2 , CO, CH_4 and CO_2).

The activity results are presented in Fig. 1. It appeared that among tested Ni/zirconia catalysts the highest H_2 yield was achieved in the case of Ni-ZR-5 and just slightly lower yield was obtained for Ni-ZR-2, whereas the lowest yield was observed for Ni-ZR-3. In every case the hydrogen yield was higher in the presence of a catalyst. The amount of CO_2 was lower in most cases when a catalyst was used, compared to the non-catalytic reaction. In contrast, the changes in the amount of CH_4 and CO obtained in catalytic and non-catalytic reactions were insignificant. The highest CH_4 yield was achieved over Ni-ZR-4.

The exact mechanism of thermal decomposition of cellulose is unknown. The depolymerized sugar unit intermediates are probably adsorbed on the metal surface, where they undergo dehydrogenation, hence the increasing hydrogen yield in the presence of a catalyst. Subsequently, the cleavage of C–O and C–C bonds can occur to form various carbonaceous products. Without external

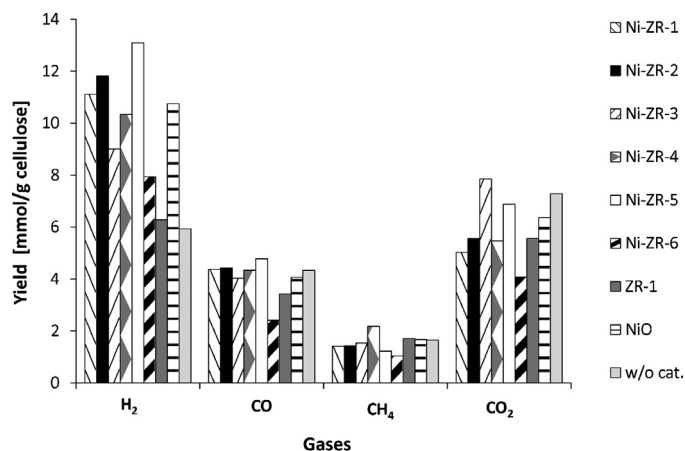
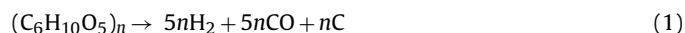


Fig. 1. Product distribution in thermal conversion of cellulose for different catalytic systems.

water or air, the reaction proceeds with oxygen deficit, according to the following simplified equation



where the formation of carbon is inevitable, and CO_2 can also be formed with further carbon release ($2CO \rightarrow CO_2 + C$). In the reaction conditions dehydration of cellulose cannot be fully excluded, as well as the presence of residual water in the starting material, hence the water-gas shift reaction might also take place to some extent with the formation of methane and higher hydrocarbons.

Nickel is known for its tendency to catalyze the C–C cleavage [4,5], and the formed cracking products can be dehydrogenated more easily, which is probably the reason for the high hydrogen yields achieved over the examined Ni catalysts except Ni-ZR-3. The latter exhibited a significantly higher CO_2 yield, which can be caused by its increased tendency to the carbon deposit formation by decomposition of carbon monoxide to CO_2 and C.

The highest activity of all the tested catalysts was observed in the first hour of the reaction, after which a significant drop of hydrogen yield was observed (Fig. 2). Despite this activity decrease, Ni-ZR-5 still exhibited the best catalytic performance during the whole time of the process. In contrast to Ni-ZR-5, non-supported NiO lost its activity to a greater extent.

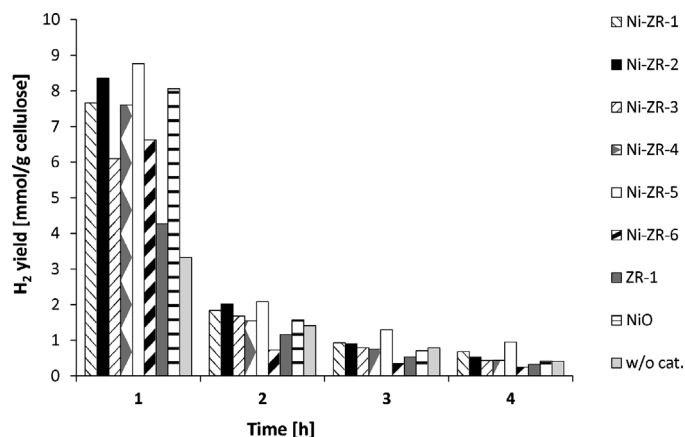


Fig. 2. Production of hydrogen in the subsequent time periods.

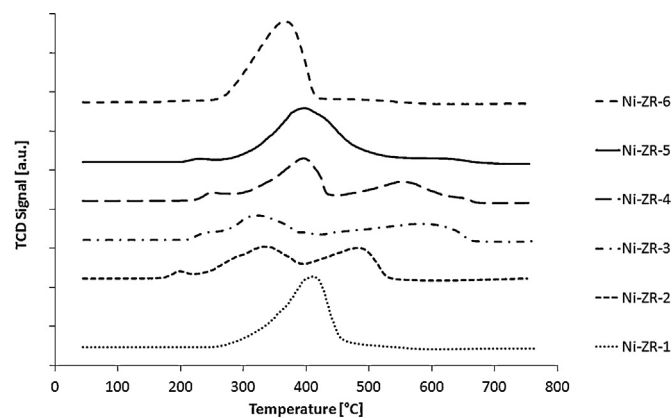


Fig. 3. TPR profiles for Ni/ZrO₂ catalysts.

3.2. Physicochemical characterization of the catalysts

3.2.1. Temperature-programmed reduction (TPR)

In order to study the reducibility of the active phase, TPR analysis was performed, the results of which are shown in Fig. 3. For Ni-ZR-1 only one sharp peak was visible with the maximum at about 400 °C, which can be probably assigned to large NiO crystallites in contact with the support. A very different reduction behavior was observed in the case of Ni-ZR-2, Ni-ZR-3 and Ni-ZR-4, where two or more reduction maxima were visible.

Ni-ZR-2 exhibited two main peaks with maxima at 330 and 480 °C, respectively, and a much smaller one at 200 °C. The latter might be attributed to the reduction of bulk NiO remaining without contact with zirconia, which is in agreement with literature [20]. The aforementioned broad peak at 330 °C was caused by low temperature reduction of highly dispersed nickel oxide, while the 480 °C peak was assigned to NiO in strong interaction with the support [21]. Similar behavior could be observed for Ni-ZR-4, although in that case the respective maxima were slightly shifted towards higher temperatures, which may indicate that NiO was dispersed more thoroughly and even more strongly interacting with the zirconia support. In the case of Ni-ZR-3, the only difference was that the high temperature peak was very broad without a clear maximum.

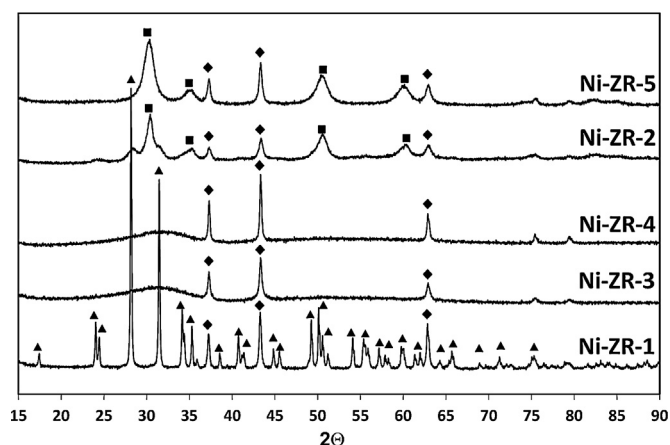
In contrast, only one main reduction peak was visible for Ni-ZR-5, although it was very broad and a shoulder of more highly interacting NiO could still be distinguished at higher temperatures up to 650 °C, just like for Ni-ZR-2, Ni-ZR-3 and Ni-ZR-4, and unlike in the case of Ni-ZR-1. The broad peak in the Ni-ZR-5 profile might suggest a relatively uniform particle size of NiO, which interacts with the support but perhaps not as strongly as in the other examined materials.

3.2.2. X-ray photoelectron spectroscopy (XPS)

XPS spectra collected from the surface of different Ni/ZrO₂ catalysts calcined at 500 °C showed in all cases the presence of principal peaks of Ni 2p_{1/2} (BE in the 871–883 range) and Ni 2p_{3/2} (BE in the 853–866 range) representative of Ni in the +2 oxidation state. It indicates that nickel occurs on the ZrO₂ surface mainly as NiO. However, minor contribution from Ni(OH)₂, whose principal peak appears at BE ~ 855.6, cannot be excluded. An analysis of calculated ratio between the intensity of signals corresponding to Zr and Ni revealed considerable differences in the composition of the surface of the catalysts prepared by various methods (Table 1). The value of Zr/Ni ratio varied in the range from 0.1 (Ni-ZR-4) to 0.6 (Ni-ZR-5). It demonstrated that during the treatment zirconia can partially migrate onto the surface of Ni crystallites. This has a great impact on the catalyst activity in the studied process. The samples distinguished by highest Zr/Ni value showed also the highest activity for

Table 1
Physicochemical properties of different Ni-zirconia systems.

Catalyst	Zirconia phase (XRD test before the reaction)	Zirconia phase (XRD test after reaction)	Average crystalline size of NiO before the reaction (nm) (XRD)	Average crystalline size of NiO after reaction (nm) (XRD)	BET ^a (m ² /g)	BET ^b (m ² /g)	BET ^c (m ² /g)	XPS Zr/Ni ratio	Pore volume (cm ³ /g)	Pore contribution (%)	Micropores	Mezopores
Ni-ZR-1	Monoclinic	Monoclinic	48.0	58.4	<5	<5	<5	0.4	0.02	5.40	76.96	—
Ni-ZR-2	Tetragonal	Monoclinic and tetragonal	18.2	28	111	58	27	0.5	0.06	4.63	88.30	—
Ni-ZR-3	Amorphous	—	36.2	—	362	200	118	0.2	0.18	7.55	90.92	—
Ni-ZR-4	Amorphous	Tetragonal	62.0	132	240	174	108	0.1	0.13	6.53	91.77	—
Ni-ZR-5	Tetragonal	Tetragonal	26.5	45	186	122	110	0.6	0.21	8.02	90.71	—
Ni-ZR-6	Monoclinic	Monoclinic	49	—	<5	<5	<5	—	—	—	—	—

^a BET of the zirconia support without metal.^b BET of Ni catalyst before reaction.^c BET of catalysts after reaction.**Fig. 4.** XRD profiles for Ni/ZrO₂ catalysts (▲, ZrO₂ monoclinic; ■, tetragonal; ◆, NiO).

hydrogen production. On the other hand the materials exhibiting small Zr/Ni values allow to produce significantly smaller amounts of hydrogen.

3.2.3. Surface characterization study

One of our aims was to prepare materials with high surface area which would be thermally stable in the reaction conditions. As it is shown in Table 1, the most stable surface was found in Ni-ZR-5, where only a very small area drop (10%) was noticed after the reaction. Such a behavior of the aforementioned catalyst was also described in the literature [19]. Thanks to the high surface area of the Ni-ZR-5 support, small NiO crystallites could also be obtained. What is more, this zirconia has also a higher contribution of tetragonal phase (Table 1 and Fig. 4), which was most probably formed thanks to the high pH value during its synthesis, which is in agreement with literature [22].

Tetragonal phase was also the main contribution in Ni-ZR-2. It possessed a relatively high surface area (111 m²/g), which was the result of applying a slow calcination temperature ramp. It is therefore clear that this surface area was also easily affected by high temperature and dropped significantly during reaction conditions (by 53%). In the samples with amorphous zirconia (Ni-ZR-3 and Ni-ZR-4) the surface drop during the reaction was also significant (41% and 38%, respectively). On their surfaces also large NiO crystallites were formed. In the case of the commercial sample (Ni-ZR-1) it is difficult to talk about its thermal stability, as its surface area was originally very low. However, with the large contribution of monoclinic phase it is clear that large NiO crystallites were formed. It is also assumed that NiO partly remained as bulk with very limited contact with zirconia. TEM images confirmed the differences in the size of NiO particles and the differences of the morphology of the investigated materials. The selected images are shown in Fig. 5.

Besides the surface area value, also the pore size can exert an influence on the catalyst activity. It appears that the most active catalyst Ni-ZR-5 exhibits a high contribution of mesopores (Table 1).

4. Discussion

In this work, we explored the possibilities of zirconia-supported nickel oxide catalysts as efficient systems for hydrogen production from cellulose. We attempted to correlate the structural changes of those materials with their catalytic performance.

The highest hydrogen yield was obtained on Ni-ZR-5. This system had the highest contribution of tetragonal phase, which was retained in the reaction conditions (Table 1). It is known that this metastable tetragonal phase can be stabilized by Ni doped into ZrO₂ and it was already reported that the highest contribution

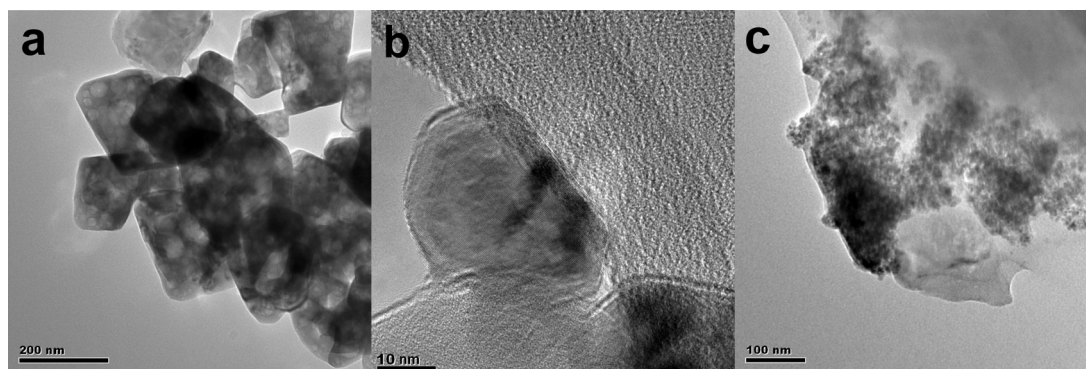


Fig. 5. TEM images of (a) Ni-ZR-3, (b) Ni-ZR-1 and (c) Ni-ZR-5.

of this phase in nickel catalysts can increase their activity [23]. This is additionally confirmed by the results obtained for Ni-ZR-2, where also the tetragonal phase was in majority at the beginning of the reaction, however after high temperature treatment two forms (monoclinic and tetragonal) were present in the sample.

On the other hand it is known that small, stable nickel particles are very active, and they can additionally change the character of the formed carbon deposit (formation of filamentous carbon is promoted, instead of graphitic encapsulating carbon) which in fact can additionally stabilize the catalytic activity so that it is not lost during the reaction time as fast as in the other cases [13].

The smallest NiO particles were obtained in the Ni-ZR-2 material, closely followed by Ni-ZR-5. Their stability was similar in the reaction conditions. However, only in one of the catalysts (Ni-ZR-5) the tetragonal phase was retained during the reaction.

Another seemingly crucial aspect is the stability of surface area. Especially in the case of Ni-ZR-5 it was managed to achieve a very high and stable surface area, which corresponds to the highest obtained hydrogen yield. This stood in contrast to Ni-ZR-2, where the surface area decreased significantly during the reaction, and which as a consequence became less active. The worst catalytic performance was exhibited by the two amorphous materials (Ni-ZR-3 and Ni-ZR-4), which had similarly unstable surface areas of zirconia and very large NiO crystallites.

A very interesting observation was made in the XPS analysis with respect to the Zr/Ni ratio. Its growth was accompanied by linearly increasing catalytic activity.

It has been described in the literature that at high temperatures a migration of zirconium ions, as well as Ni or NiO, takes place [11,24]. When we correlate it with the types of ZrO₂ crystalline phases, according to the XPS results the highest migration tendency is exhibited by the tetragonal phase of zirconia, followed by the monoclinic one, with amorphous ZrO₂ showing the lowest migration. On the other hand it is difficult to elucidate any relationship between this migration and the surface area. It is clear however that a closer NiO–ZrO₂ contact facilitates reaching higher activity values, which can be connected with the aforementioned easier stabilization of zirconium tetragonal phase by Ni, or the character of carbon formed. High activity attributed to tetragonal phase presence was already suggested in literature in reactions of steam reforming of glycerol for zirconia based systems [25,26].

The XRD analysis has not revealed any clear evidence of formation of alloys in the samples which exhibited the highest migration degree after the reaction. It seems therefore that the chemical forms of Ni and Zr do not change. Although the alloy formation cannot be fully excluded, its amount would have to be too low, or its crystalline size too small to be detected by XRD.

In order to examine the significance of the alloy presence in the catalytic reaction, one sample (Ni-ZR-6) was calcined at a much higher temperature (900 °C), thus facilitating the possible conditions of alloy formation. Over such prepared catalyst only a small hydrogen yield was achieved. Catalytic tests of ZrO₂ and NiO alone were performed as well. For ZrO₂ there was no activity observed, while NiO in the first hour of the reaction exhibited some activity, which however declined very quickly, probably due to the fast formation of carbon deposit.

5. Conclusions

The catalytic performance of several differently prepared Ni/ZrO₂ systems in the conversion of cellulose to hydrogen was investigated. Several factors, such as the crystalline phase type of the support, the NiO particle size, as well as the surface area stability and the tendency of zirconia migration to the nickel surface, were found to exert a significant impact on the catalytic activity. The highest hydrogen yield was obtained over the Ni-ZR-5 catalyst, which contains tetragonal zirconia and small NiO crystallites, retains a stable surface area in the reaction conditions and exhibits a high degree of zirconia migration to the active phase. It appears that the combination of the above parameters is responsible for the increased contact between the ZrO₂ and NiO phases, which is beneficial for the enhanced catalytic activity and hydrogen yield.

Acknowledgements

The authors are thankful to Dr. Waldemar Maniukiewicz for performing XRD measurements, and gratefully acknowledge that this work was financially supported by the National Science Center (Poland) – project 2011/03/B/ST5/03270.

References

- [1] A.M. Ruppert, K. Weinberg, R. Palkovits, *Angewandte Chemie International Edition* 51 (11) (2012) 2564–2601.
- [2] R.N. Widyanyingrum, T.L. Church, M. Zhao, A.T. Harris, *International Journal of Hydrogen Energy* 37 (2012) 9590–9601.
- [3] R.C. Saxena, D. Seal, S. Kumar, H.B. Goyal, *Renewable and Sustainable Energy Reviews* 12 (2008) 1909–1927.
- [4] D. Swierczynski, S. Libs, C. Courson, A. Kiennemann, *Applied Catalysis B* 74 (2007) 211–222.
- [5] J. Han, H. Kim, *Renewable and Sustainable Energy Reviews* 12 (2008) 397–416.
- [6] E.C. Wanat, K. Venkataraman, L.D. Schmidt, *Applied Catalysis A* 276 (2004) 155–162.
- [7] S. Freni, S. Cavallaro, N. Mondello, L. Spadaro, F. Frusteri, *Journal of Power Sources* 108 (2002) 53–57.
- [8] K. Urasaki, K. Tokunaga, Y. Sekine, M. Matsuoka, E. Kikuchi, *Catalysis Communications* 9 (2008) 600–604.
- [9] H.M. Swaan, V.C.H. Kroll, G.A. Martin, C. Mirodatos, *Catalysis Today* 21 (1994) 571–578.

- [10] M.H. Youn, J.G. Seo, J.C. Jung, S. Park, D.R. Park, S.-B. Lee, I.K. Song, *Catalysis Today* 146 (2009) 57–62.
- [11] A.M. Ruppert, T. Paryjczak, *Applied Catalysis A* 320 (2007) 80–90.
- [12] A. Iriondo, J.F. Cambra, M.B. Guez, V.L. Barrio, J. Requies, M.C. Sanchez-Sanchez, R.M. Navarro, *International Journal of Hydrogen Energy* 37 (2012) 7084–7093.
- [13] W.-T. Zheng, K.-Q. Sun, H.-M. Liu, Y. Liang, B.-Q. Xu, *International Journal of Hydrogen Energy* 37 (2012) 11735–11747.
- [14] M. Watanabe, H. Inomata, K. Arai, *Biomass and Bioenergy* 22 (2002) 405–410.
- [15] M. Inaba, K. Murata, M. Saito, I. Takahara, *Energy and Fuels* 20 (2) (2006) 432–438.
- [16] J. Matras, M. Niewiadomski, A. Ruppert, J. Grams, *Kinetics and Catalysis* 53 (5) (2012) 565–569.
- [17] A. Ruppert, J. Matras, M. Niewiadomski, J. Kałużna-Czaplińska, P. Przybysz, J. Grams, J. Rynkowski, P. in, G. Da Costa, A. Djega-Mariadassou, Krztoń (Eds.), *Catalysis for Environment Depollution, Renewable Energy and Clean Fuels*, UKIP, Gliwice, 2011, pp. 29–33.
- [18] M. Rezaei, S.M. Alavi, S. Sahebdehfar, P. Bai, X. Liu, Z.-F. Yan, *Applied Catalysis B* 77 (2008) 346–354.
- [19] S. Guerrero, P. Araya, E.E. Wolf, *Applied Catalysis A* 298 (2006) 243–253.
- [20] T.L. Lai, Y.Y. Shu, G.L. Huang, C.C. Lee, C.B. Wang, *Journal of Alloys and Compounds* 450 (1–2) (2008) 318–322.
- [21] Q. Liu, X. Dong, X. Mo, W. Lin, *Journal of Natural Gas Chemistry* 17 (2008) 268–272.
- [22] G.K. Chuah, S.H. Liu, S. Jaenicke, J. Li, *Microporous and Mesoporous Materials* 39 (2000) 381–392.
- [23] M. Yamasaki, H. Habazaki, T. Yoshida, M. Komori, K. Shimamura, E. Akiyama, A. Kawashima, K. Asami, K. Hashimoto, *Applied Catalysis A* 163 (1997) 187.
- [24] P.M. Delaforce, J.A. Yeomans, N.C. Filkin, G.J. Wright, R.C. Thomson, *Journal of the American Ceramic Society* 90 (3) (2007) 918–924.
- [25] J.G. Seo, M.H. Youn, I.K. Song, *Journal of Molecular Catalysis A* 268 (2007) 9–14.
- [26] J.G. Seo, M.H. Youn, J.C. Jung, K.M. Cho, S. Park, I.K. Song, *Catalysis Today* 138 (2008) 130–134.